NRL Memorandum Report 4767

Return-Current-Driven Instabilities of Propagating Electron Beams

HAN S. UHM

Naval Surface Weapons Center
Silver Spring, MD 20910

MARTIN LAMPE

Plasma Theory Branch
Plasma Physics Division

March 5, 1982

This research was supported in part by the Independent Research Fund at the Naval Surface Weapons Center and in part by Defense Advanced Research Projects Agency (DoD) under ARPA Orders No. 3718, Amendment 32, and No. 4395, Amendment 1.

NAVAL RESEARCH LABORATORY
Washington, D.C.

SECURITY CLASSIFICATION OF THIS PAGE (When Data Entered)

REPORT DOCUMENTATION PAGE

READ INSTRUCTIONS BEFORE COMPLETING FORM

1. REPORT NUMBER: NRL Memorandum Report 4767
2. GOVT ACCESSION NO.: AD-A111 911
3. RECIPIENT'S CATALOG NUMBER:

4. TITLE (and Subtitle): RETURN-CURRENT-DRIVEN INSTABILITIES OF PROPAGATING ELECTRON BEAMS
5. TYPE OF REPORT & PERIOD COVERED: Interim report on a continuing NRL problem.
6. PERFORMING ORG. REPORT NUMBER:

7. AUTHOR(s): Han S. Uhm* and Martin Lampe
8. CONTRACT OR GRANT NUMBER(s): 4395 ARPA O 3718

9. PERFORMING ORGANIZATION NAME AND ADDRESS: Naval Research Laboratory, Washington, DC 20375
10. PROGRAM ELEMENT, PROJECT, TASK AREA & WORK UNIT NUMBERS: 47-0900-0-2

11. CONTROLLING OFFICE NAME AND ADDRESS: Defense Advanced Research Projects Agency, Arlington, VA 22209
12. REPORT DATE: March 5, 1982
13. NUMBER OF PAGES: 33

14. MONITORING AGENCY NAME & ADDRESS(if different from Controlling Office): Naval Surface Weapons Center, Silver Spring, MD 20910
15. SECURITY CLASS. (of this report): UNCLASSIFIED
15a. DECLASSIFICATION/DOWNGRADING SCHEDULE:

16. DISTRIBUTION STATEMENT (of this Report)

Approved for public release; distribution unlimited.

17. DISTRIBUTION STATEMENT (of the abstract entered in Block 20, if different from Report)

18. SUPPLEMENTARY NOTES

*Present address: Naval Surface Weapons Center, Silver Spring, MD 20910

This research was supported in part by the Independent Research Fund at the Naval Surface Weapons Center and in part by Defense Advanced Research Projects Agency (DoD) under ARPA Orders No. 3718, Amendment 32, and No. 4395, Amendment 1.

19. KEY WORDS (Continue on reverse side if necessary and identify by block number)

Beam propagation
Relativistic electron beams
Charged particle beams
Hose instability
Sausage instability
Hollowing instability
Filamentation instabilities

omega
omega tau sub d <<
< or =

20. ABSTRACT (Continue on reverse side if necessary and identify by block number)

A stability analysis is performed for the first nine transverse modes (azimuthal mode number plus radial mode number ≤ 3) of a self-pinched relativistic electron beam propagating in a collisional plasma. Only frequencies ω in the range $\omega\tau_d \ll 1$ are considered, where τ_d is the dipole magnetic decay length. For such modes, the presence of plasma return current is the only destabilizing mechanism. Paraxial flow, space charge

(Continues) → OVER

tau sub d

DD FORM 1 JAN 73 1473 EDITION OF 1 NOV 65 IS OBSOLETE
S/N 0102-014-6601

SECURITY CLASSIFICATION OF THIS PAGE (When Data Entered)

20. ABSTRACT (Continued)

neutrality, and a flat radial profile of beam density are also assumed. Within these limitations an exact analysis of the linearized Vlasov stability problem is carried out in closed form. For each mode, the instability threshold, growth rate, and conditions for oscillatory vs. pure growth are determined. For beams with a moderate return current fraction, the hose, sausage and axial hollowing modes appear to be particularly dangerous.

CONTENTS

RETURN-CURRENT-DRIVEN INSTABILITIES OF PROPAGATING ELECTRON BEAMS

I. Introduction

In recent years, there have been many investigations[1-7] of the resistive instabilities of a self-pinched relativistic electron beam propagating through a collisional plasma. These instabilities are driven by two mechanisms: (i) resistive phase lags due to magnetic diffusion and/or (ii) magnetic repulsion between the beam current and the plasma return current. The first mechanism is in some ways more delicate and is particularly sensitive to the details of a theoretical model, since the destabilizing effect of resistive phase lags between the perturbed beam current and the perturbed currents induced in the plasma can be neutralized by the stabilizing effect of phase mixing among beam particles with different betatron frequency.[3,4,6,7] The distribution of betatron frequencies depends on the degree of anharmonicity of the self-pinch, and therefore on the radial profile of net current density $J_{no}(r)$; all particles have the same betatron frequency if $J_{no}(r)$ is flat. Thus it is important in treating resistive phase lag effects to model the beam current profile $J_{bo}(r)$ and the return current profile $J_{po}(r)$ with appropriate rounded shapes and to include phase mixing in a realistic way.[3,4,6,7] When this is done, the hose mode is found to be unstable even if there is no equilibrium return current. However it is widely believed that for typical rounded beam profiles such as the Bennett profile none of the other modes are destabilized by resistive phase lag effects alone when phase mixing is modeled realistically; these modes become unstable only when the return current exceeds a threshold value.

The purpose of the present paper is to investigate the destabilizing effect of plasma return current on a variety of beam modes with azimuthal mode number $0 \leq n \leq 3$ and radial mode number in the range $0 \leq n \leq 3$. We exclude the

Manuscript submitted December 29, 1981.

effect of magnetic phase lags (and considerably simplify the analysis) by considering only frequencies in the range $\omega\tau_d \ll 1$, where τ_d is the dipole magnetic decay time. Instabilities in this frequency range, due entirely to plasma return current, are not stabilized by phase mixing, and are only moderately sensitive to the profile of $J_{bo}(r)$, as is shown in Ref. 8 for the sausage mode ($m = 0$, $n = 1$). We consider here the simplest beam equilibrium model, in which $J_{bo}(r)$ is flat. We also assume here that the conductivity of the background plasma is high enough to assure space charge neutrality. Within these constraints, we are able to formulate a Vlasov-Maxwell treatment of the instabilities, and solve it in closed form.

The present paper is a direct extension of our previous work[5] to a wider selection of modes. Analysis of the higher modes considered here is very complicated, but the present analysis is tremendously simplified by the assumptions of charge neutrality and $\omega\tau_d \ll 1$; otherwise, the equilibrium considered is similar to that of Ref. 5. With slight modifications, the results of this paper can also be applied to ion beam transport in an inertial confinement fusion reactor vessel.

The outline of the paper is as follows. The equilibrium is specified in Sec. II. A normal mode treatment of the linearized Vlasov-Maxwell stability problem is formulated in Sec. III and the method of exact solution is outlined. The dispersion relations for all unstable modes with $0 \leq n \leq 3$, $1 \leq m + n \leq 3$ are calculated in Sec. IV in terms of the degree of current neutralization, and are discussed with emphasis on instability thresholds and transitions between oscillatory and purely-growing instability.

II. Equilibrium Model

We consider a self-pinched relativistic electron beam propagating through a collision-dominated background plasma. Cylindrical polar coordinates (r,θ,z) are used, with the z axis along the axis of symmetry. Both the beam and plasma, in equilibrium, are taken to be azimuthally symmetric ($\partial/\partial\theta = 0$), infinitely long, and axially symmetric ($\partial/\partial z = 0$). There is no external magnetic field, and we assume that the plasma conductivity $\sigma(r)$ is large enough to assure space charge neutrality out to a radius R_c much larger than the beam radius R_b. This requires only a weak conductivity,

$$4\pi\sigma(r)R_b > c, \qquad 0 < r < R_b, \tag{1a}$$

$$4\pi\sigma(r)r > c, \qquad R_b < r < R_c, \tag{1b}$$

and is usually satisfied when a beam propagates into pre-ionized plasma, or even into neutral gas of density $\gtrsim 1$ torr (except at the beam head). We also assume that

$$\nu/\gamma_b \equiv \frac{I_b e}{Mc^3(\gamma_b^2-1)^{1/2}} \equiv \frac{I_b}{17\,(\gamma_b^2-1)^{1/2}\,\mathrm{kAmp}} \ll 1, \tag{2}$$

where ν is Budker's parameter, I_b the beam current, $-e$ and M the charge and mass of the electron, c the speed of light in vacuo, and γ_b the beam relativistic factor. A beam satisfying Eq. (2) is paraxial, i.e. perpendicular velocities $v_\perp$ are much smaller than axial velocities.

We consider the particular equilibrium distribution function

$$f_{bo}(H,P_z) = \frac{n_{bo}}{2\pi\gamma_b M}\,\delta(H - \tilde{\gamma}Mc^2)\,\delta(P_z - \tilde{\gamma}M\beta_b c) \tag{3}$$

where $H = (M^2c^4 + c^2p^2)^{\frac{1}{2}}$ is the particle energy, $P_z = p_z - eA_o(r)/c$ is the axial canonical momentum, $A_o(r)$ is the axial component of vector potential from which the equilibrium self-pinch field $\underset{\sim}{B}_\theta(r)$ is derived, $\underset{\sim}{p} = (p_r, p_\theta, p_z)$ is the mechanical momentum, γ_b is defined[9] by $\gamma_b \equiv (1 + P_z^2/M^2c^2)^{1/2}$, and n_{bo} and $\tilde{\gamma}$ are constants. For a paraxial beam, $\tilde{\gamma}$ is only slightly larger than γ_b. As a consequence of (2), $eA_o/c \ll p_z$ and the axial velocity v_z is nearly constant and the same for all particles,

$$v_z \approx \beta_b c. \tag{4}$$

We further assume that the equilibrium plasma return current $J_{po}(r)$ has the same profile as the beam current $J_{bo}(r)$,

$$J_{po}(r) = -f\,J_{bo}(r), \tag{5}$$

where the fractional current neutralization f is a constant with $0 \leq f \leq 1$. From (2), (3) and (5) it follows that the equilibrium beam density profile is

$$n_{bo}(r) = \int d^3p f_{bo} = \begin{cases} n_{bo}, & 0 \leq r < R_b \\ 0, & R_b \leq r, \end{cases} \tag{6}$$

where

$$R_b^2 = 2c^2(\tilde{\gamma} - \gamma_b)\,\gamma_b^{-1}\,\omega_\beta^{-2} \tag{7}$$

is the beam radius squared,

$$\omega_\beta^2 \equiv \frac{1}{2}\,\omega_{pb}^2\beta_b^2\,(1-f) \equiv 2\pi n_{bo}e^2\beta_b^2\,(1-f)/\gamma_b M \qquad (8)$$

is the betatron frequency squared, and ω_{pb} is the plasma frequency.

The conductivity profile $\sigma(r)$ does not appear explicitly in either the equilibrium or perturbation calculations in this paper, but it can be inferred from conditions (1) and (5) that $\sigma(r)$ is relatively large and nearly independent of r for $0 \leq r \leq R_b$, and then falls to a much smaller value consistent with (1) for $R_b < r < R_c$.

The properties of this equilibrium and related equilibria are discussed in more detail in Refs. 4 and 5.

III. Linearized Vlasov Analysis

As discussed in Sec. I, our aim in this paper is to determine the stability properties of a number of modes, all of which (except for the hose mode) are destabilized primarily by the presence of an equilibrium return current. To eliminate the additional destabilizing (and complicating) effects of resistive phase lags due to magnetic diffusion, we consider only modes that satisfy

$$|\omega|\ \tau_d \equiv \pi\sigma(0)R_b^2\ |\omega|/2c^2 << 1, \tag{9}$$

where ω is the eigenfrequency and τ_d is "dipole" magnetic decay time, which actually is a roughly characteristic decay time for magnetic field patterns corresponding to any of the first few perturbation modes. We adopt a normal mode approach in which any perturbed quantity $\Phi_1(\underset{\sim}{x},t)$ with azimuthal mode number m is represented as

$$\Phi_1(\underset{\sim}{x},t) = \hat{\Phi}(r)\exp[i(m\theta+kz-\omega t)], \tag{10}$$

where k is the axial wavenumber. Introducing the variable[4,5] $\tau \equiv t - z/\beta_b c$, this Fourier representation is rewritten as

$$\Phi_1(\underset{\sim}{x},\ t) = \hat{\Phi}(r)\exp[i(m\theta-\omega\tau-\Omega z/\beta_b c)], \tag{11}$$

where $\Omega \equiv \omega - k\beta_b c$ is the shifted frequency "seen" by a beam particle (but not in the sense of a Lorentz transformation).

Conditions (1) and (9) together indicate that c/ω is long compared to the beam radius

$$|\omega| << c/R_b, \tag{12a}$$

and the subsequent analysis clearly indicates that when (2) is satisfied

$$|\Omega| \lesssim \text{few} \cdot \omega_{pb}\beta_b \ll c/R_b \tag{12b}$$

for all modes. It follows from (1) and (12a) that for $r \leq R_b$,

$$4\pi\sigma \gg |\omega|, \tag{13}$$

which guarantees that the perturbed beam space charge field is also completely neutralized by the plasma. In the context of (1), (2), (12), and (13), only magnetic fields $\hat{\underset{\sim}{B}}_\perp$ in the (r,θ) plane play any significant role in the electrodynamics. These fields can be derived from the axial component $\hat{A}$ of the perturbed vector potential, and Maxwell's equations reduce to Ampere's law for $\hat{A}$. Moreover, (9) indicates that the perturbed plasma current can be neglected, and Ampere's law thus reduces to

$$\left(\frac{1}{r}\frac{d}{dr}\, r\, \frac{d}{dr} - \frac{m^2}{r^2} \right) \hat{A}(r) = -\frac{4\pi}{c}\, \hat{J}_b(r) \tag{14}$$

where $\hat{J}_b(r)$ is the axial component of the perturbed beam current density.

Using the Fourier representation (11), the perturbed beam current $\hat{J}_b(r)$ is expressed as a moment of the perturbed beam distribution function $f_{b1}(\underset{\sim}{x}_\perp, \underset{\sim}{p}, \tau, z)$,

$$\hat{J}_b(r) = -\, e\, \exp[i(-m\theta + \omega\tau + \Omega z/\beta_b c)] \int d^3p v_z f_{b1}(\underset{\sim}{x}_\perp, \underset{\sim}{p}, \tau, z), \tag{15}$$

and f_{b1} is formally evaluated, in standard Vlasov fashion, as an integral over unperturbed electron trajectories,

$$f_{b1}(\underset{\sim}{x}_\perp, \underset{\sim}{p}, \tau, z) = e \int_{-\infty}^{0} d\tilde{z} \exp\left(- \frac{i\Omega\tilde{z}}{\beta_b c} \right) \frac{\underset{\sim}{v}' \times \underset{\sim}{B}_1}{c} \cdot \frac{\partial}{\partial \underset{\sim}{p}} f_{bo}. \qquad (16)$$

In Eq. (16), the unperturbed particle trajectory is specified as a function of z, with $\underset{\sim}{x}_\perp' \equiv \underset{\sim}{x}_\perp(z-\tilde{z})$, $\underset{\sim}{v}' \equiv \underset{\sim}{v}(z-\tilde{z})$ being the coordinates in the (r,θ) plane and velocity, at an earlier time, of a particle with coordinates and velocity $\underset{\sim}{x}_\perp, \underset{\sim}{v}$ at z. It is assumed that $\mathrm{Im}\Omega > 0$. We note that $\hat{B} = \nabla \times \hat{A}$, and use (2) and (4), from which it follows that $v_\perp << v_z$, and that v_z and τ are essentially constant over a particle trajectory. We can then reduce Eqs. (14) - (16) to the form

$$(1 - f)\left(\frac{1}{r}\frac{d}{dr} r \frac{d}{dr} - \frac{m^2}{r^2} \right) \hat{A}(r)$$

$$= - (2/R_b)\, \delta(r - R_b) \left[\hat{A}(R_b) + \Omega \hat{I}(R_b, p_o) \right]$$

$$- 4\gamma_b^2 M^2 \Omega \omega_\beta^2 \Theta(R_b - r) \left(\partial \hat{I}/\partial p_\perp^2\right)_{p_\perp = p_o}, \qquad (17a)$$

where $\hat{I}(r,p_\perp)$ is the orbit integral

$$\hat{I}(r,p_\perp) \equiv i \int_0^{2\pi} (d\phi/2\pi) \int_{-\infty}^{0} d\tilde{z}\, A(r') \exp[im(\theta' - \theta) - i\Omega\tilde{z}/\beta_b c], \qquad (17b)$$

and

$$\Theta(x) \equiv \begin{cases} 1, & x > 0 \\ 0, & x < 0 \end{cases} \qquad (18)$$

is the step function. We have introduced polar coordinates $(p_\perp, \phi)$ for momentum,

and have defined

$$p_o^2(r) \equiv \gamma_b M^2 \omega_\beta^2 (R_b^2 - r^2). \tag{19}$$

When supplemented by the boundary conditions required at r = 0 for cylindrical symmetry,

$$[d\tilde{A}/dr]_{r=0} = 0, \qquad m = 0 \tag{20a}$$

$$\hat{A}(0) = 0, \qquad m > 1 \tag{20b}$$

and metallic wall boundary conditions at radius $R_c > R_b$,

$$\hat{A}(R_c) = 0, \tag{20c}$$

Eqs. (17) completely specify the eigenvalue problem for frequency Ω.

For the equilibrium under consideration, with J_{bo} and J_{po} uniform out to $r = R_b$, the unperturbed electron orbits in the (r , θ) plane are ellipses, and can be specified in the closed form

$$x'(\tilde{z}) = \frac{p_\perp}{\gamma_b M \omega_\beta} \cos\phi \sin\left(\frac{\omega_\beta \tilde{z}}{\beta_b c}\right) + r\cos\theta\cos\left(\frac{\omega_\beta \tilde{z}}{\beta_b c}\right), \tag{21a}$$

$$y'(\tilde{z}) = \frac{p_\perp}{\gamma_b M \omega_\beta} \sin\theta \sin\left(\frac{\omega_\beta \tilde{z}}{\beta_b c}\right) + r\sin\theta\cos\left(\frac{\omega_\beta \tilde{z}}{\beta_b c}\right). \tag{21b}$$

Given the simple orbits (21), exact solutions to Eqs. (17) and (20) are found in the form of polynomials

$$\hat{A}(r) = r^m \sum_{j=0}^{n} a_j r^{2j}/R_b^{2j}, \qquad 0 \le r \le R_b, \tag{22a}$$

$$\hat{A}(r) = [\ell n(r/R_c)/\ell n(R_b/R_c)] \sum_{j=0}^{n} a_j, \qquad R_b \le r \le R_c,\ m = 0, \tag{22b}$$

$$\hat{A}(r) = R_b^{2m}(R_b^{2m} - R_c^{2m})^{-1}(r^m - R_c^{2m} r^{-m}) \sum_{j=0}^{n} a_j, \qquad R_b \le r \le R_c,\ m \ge 1. \tag{22c}$$

The integer n is the radial mode number, and can take any value. The coefficients a_j are functions of Ω as well as of the mode number (m,n). The determination of the coefficients a_j and of the dispersion relation is a straightforward but lengthy algebraic exercise, for which the degree of complexity increases rapidly with increasing mode numbers.

As an example, we shall outline the solution for the case of the axisymmetric modes with m = 0, n ≤ 3. The eigenfunctions are of the form

$$\hat{A}(r) = \sum_{j=0}^{3} a_j r^{2j}/R_b^{2j}, \qquad 0 \le r \le R_b, \tag{23a}$$

$$\hat{A}(r) = [\ell n(r/R_c)/\ell n(R_b/R_c)] \sum_{j=0}^{3} a_j, \qquad R_b \le r \le R_c. \tag{23b}$$

We first substitute (23a) and (21) into (17b) and evaluate the orbit integral $\hat{I}$ in terms of Ω and the coefficients a_j. This part of the calculation is tedious, but can be carried out in closed form. Next we substitute (23) into (17a) and solve (17) inside the beam. Finally, we apply an appropriate boundary condition at $r = R_b$, determined by multiplying Eq. (17a) by r and integrating over $R_b - \varepsilon \le r \le R_b + \varepsilon$, with $\varepsilon \to 0$. The result is a matrix equation of the form

$$\begin{pmatrix} \chi_{00} & \chi_{01} & \chi_{02} & \chi_{03} \\ 0 & \chi_{11} & \chi_{12} & \chi_{13} \\ 0 & 0 & \chi_{22} & \chi_{23} \\ 0 & 0 & 0 & \chi_{33} \end{pmatrix} \begin{pmatrix} a_0 \\ a_1 \\ a_2 \\ a_3 \end{pmatrix} = 0 \qquad (24)$$

with matrix elements

$$\chi_{00} = [\ell n(R_b/R_c)]^{-1}, \qquad (25a)$$

$$\chi_{01} = \chi_{00} + 2\ (\xi_1 - 1), \qquad (25b)$$

$$\chi_{02} = \chi_{00} + 4\xi_1\ (6\xi_2 + 1) - 4, \qquad (25c)$$

$$\chi_{03} = \chi_{00} + 6\xi_1\ (120\xi_2\xi_3 + 12\xi_2 + 1) - 6, \qquad (25d)$$

$$\chi_{11} = \xi_1 - 1, \qquad (25e)$$

$$\chi_{12} = -\ 24\xi_1\xi_2, \qquad (25f)$$

$$\chi_{13} = 1080\xi_1\xi_2\xi_3, \qquad (25g)$$

$$\chi_{22} = \xi_1\ (18\xi_2 + 1) - 1, \qquad (25h)$$

$$\chi_{23} = (9/5)\ (\chi_{22} - \chi_{33}) \qquad (25i)$$

$$\chi_{33} = \xi_1(1200\xi_2\xi_3 + 48\xi_2 + 1) - 1, \qquad (25j)$$

where the ξ's are susceptibility functions, given by

$$\xi_1 = -\omega_{pb}^2 \beta_b^2 (\Omega^2 - 4\omega_\beta^2)^{-1}, \tag{26a}$$

$$\xi_2 = \omega_\beta^2 (\Omega^2 - 16\omega_\beta^2)^{-1}, \tag{26b}$$

$$\xi_3 = \omega_\beta^2 (\Omega^2 - 36\omega_\beta^2)^{-1}. \tag{26c}$$

According to Eq. (24), the dispersion relations for the modes with radial mode number j are specified by the conditions

$$\chi_{jj} = 0, \qquad j = 1, 2, 3. \tag{27}$$

Since χ_{jj} is generally a polynomial in Ω^2, modes occur in pairs $\pm \Omega$, and in general there are several distinct pairs of modes with azimuthal and radial mode numbers (m,j). Because of condition (9), we have effectively specialized to the case $\omega = 0$; thus our "dispersion relation" specifies Ω as a function of the only other free parameter, f. To find the eigenfunction for any mode, the matrix equation (24) is solved for the a_j, using the previously determined value of Ω to evaluate the matrix elements χ_{ij}.

IV. Stability Analysis

A. Results

From Eqs. (24)-(27), the dispersion relations for the axisymmetric (m = 0) modes are

$$\bar{\Omega}^2 = 1 - 2f \tag{28}$$

for the m = 0, n = 1 sausage mode,

$$\bar{\Omega}^4 - (10f_e - 1)\,\bar{\Omega}^2 + f_e\,(16\,f_e + 1) = 0 \tag{29}$$

for the m = 0, n = 2 hollowing mode, and

$$(\bar{\Omega}^2 - 2f_e)\,(\bar{\Omega}^2 - 8\,f_e)\,(\bar{\Omega}^2 - 18\,f_e) + (\bar{\Omega}^2 - 8\,f_e)\,(\bar{\Omega}^2 - 18\,f_e)$$

$$+ 24\,f_e\,(\bar{\Omega}^2 - 18\,f_e) + 300\,f_e^2 = 0 \tag{30}$$

for the m = 0, n = 3 mode, where we have introduced the notation

$$f_e \equiv 1 - f, \tag{31}$$

$$\bar{\Omega} \equiv \Omega/\omega_{pb}\beta_b \equiv 2\Omega f_e/\omega_\beta. \tag{32}$$

In similar fashion, we have calculated the dispersion relations for the modes (m=1; n=0,1,2), (m=2; n=0,1) and (m=3,n=0). For convenience, we list all of these results here:

$$(1,\,0): \quad \bar{\Omega}^2 = -f \qquad \text{(hose mode)}, \tag{33}$$

$$(1,\ 1): \quad \bar{\Omega}^4 - (5f_e - 1)\,\bar{\Omega}^2 + (9/4)f_e^2 = 0, \tag{34}$$

$$(1,\ 2): \quad (2\,\bar{\Omega}^2 - 9\,f_e)\,(2\,\bar{\Omega}^2 - 25\,f_e) + 4\,\bar{\Omega}^2 = 0, \tag{35}$$

$$(2,\ 0): \quad 2\,\bar{\Omega}^2 = 4f_e - 1, \tag{36}$$

$$(2,\ 1): \quad \bar{\Omega}^2 = 8f_e - 1, \tag{37}$$

$$(3,\ 0): \quad 4\,\bar{\Omega}^4 - 2(10f_e - 1)\,\bar{\Omega}^2 + 3\,f_e\,(1 + 3f_e) = 0. \tag{38}$$

The dispersion relations, i.e. the growth rate Ω_i and oscillation frequency Ω_r as functions of f, are plotted in Fig. 1 for the m = 0 modes, in Fig. 2 for the m = 1 modes, and in Fig. 3 for the m = 2 and m = 3 modes, and will be discussed in the next section.

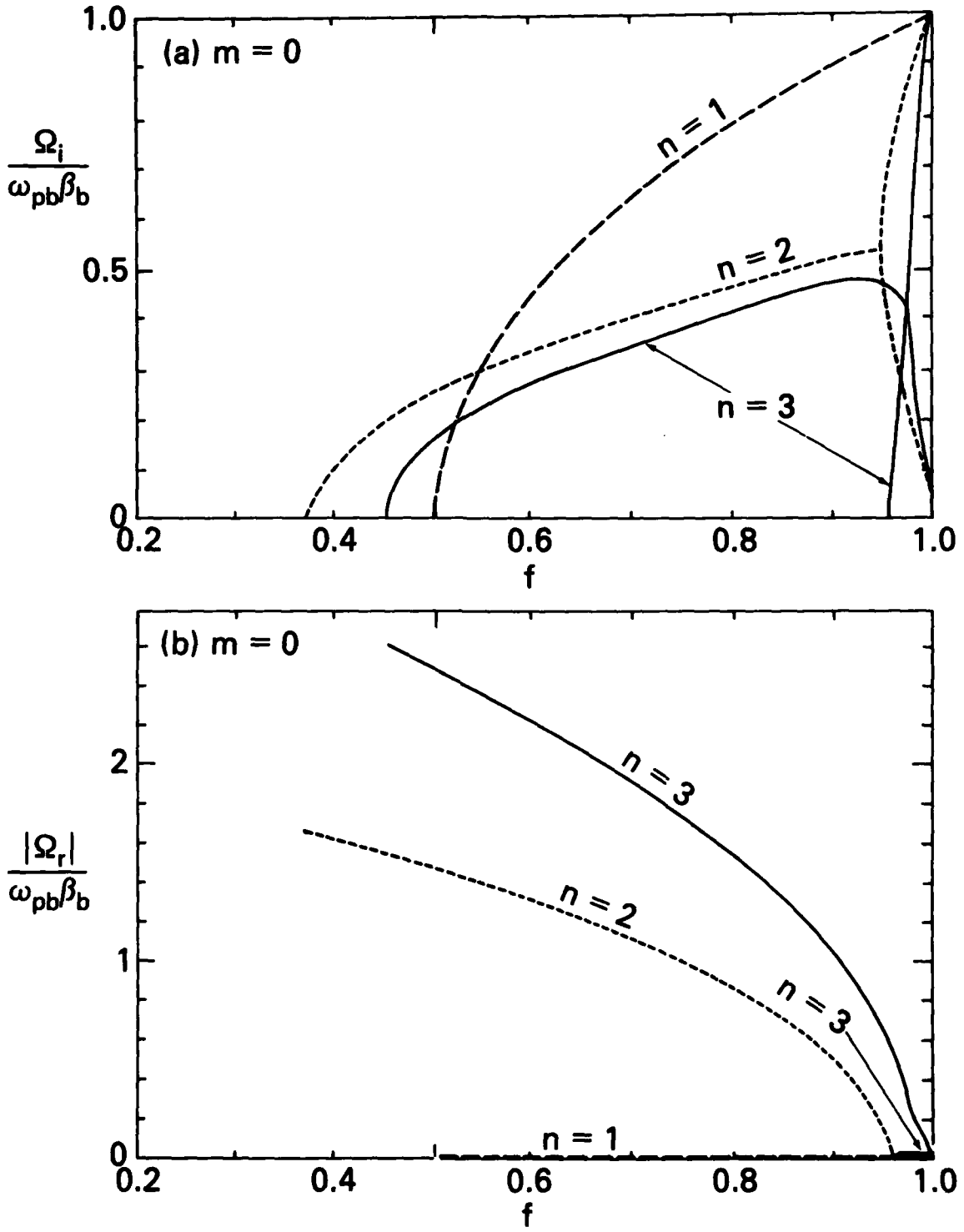

Fig. 1 — Plots of normalized (a) growth rate Ω_i and (b) shifted real frequency Ω_r versus f [Eqs. (28) — (30)] for the azimuthally symmetric perturbations (m = 0).

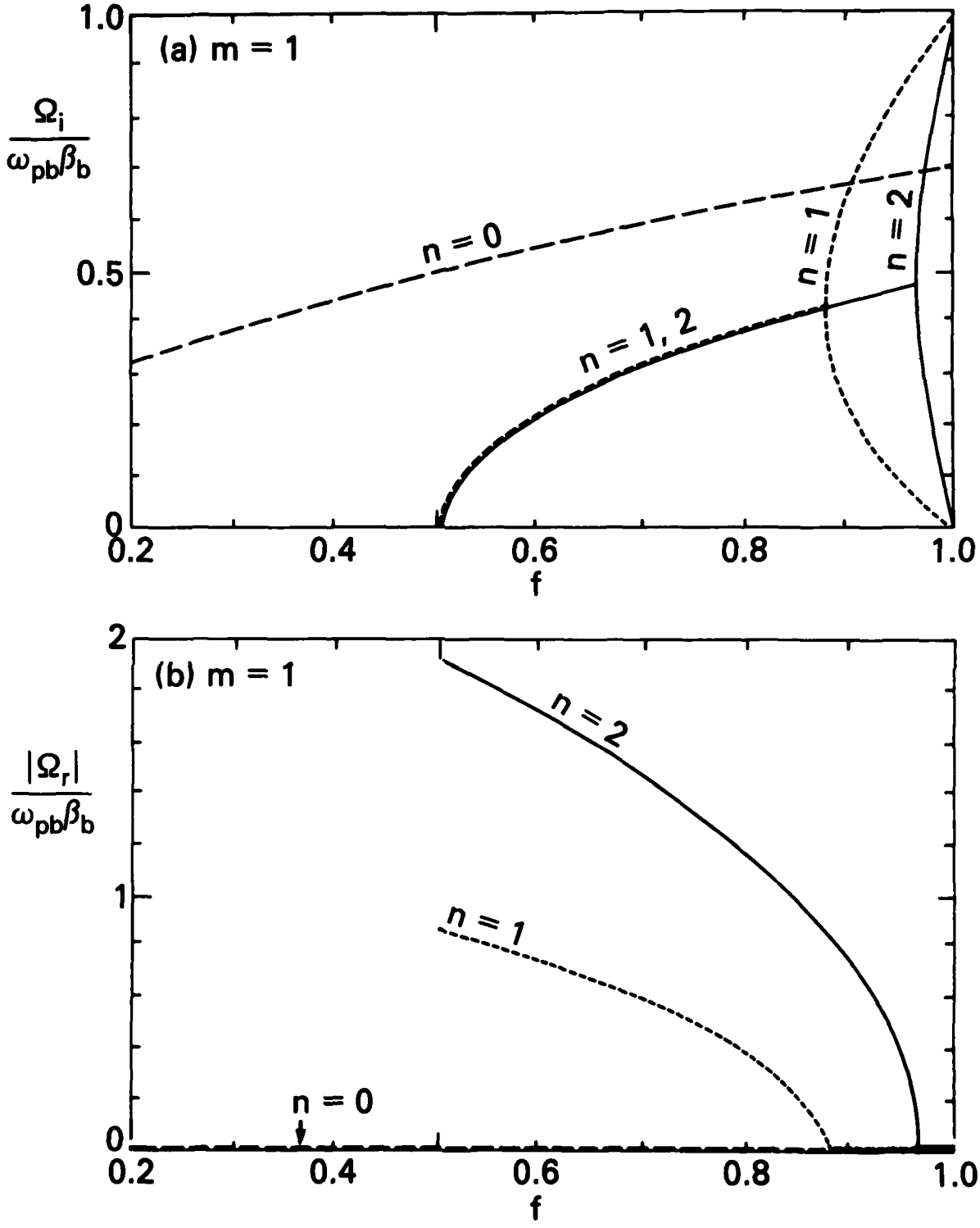

Fig. 2 — Plots of normalized (a) growth rate Ω_i and (b) shifted real frequency Ω_r versus f [Eqs. (33) — (35)] for the m = 1 modes with radial mode number n = 0 to 2.

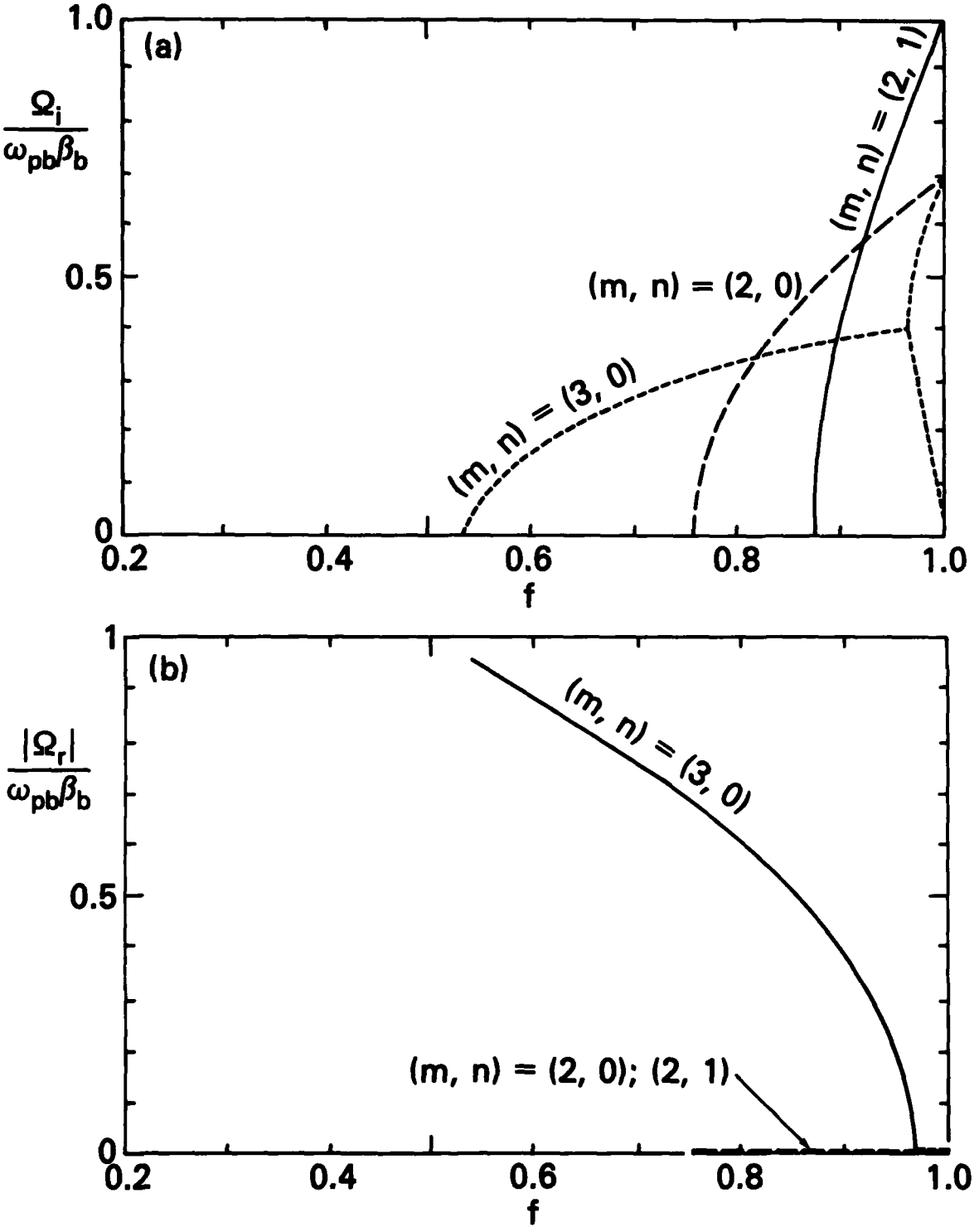

Fig. 3 — Plots of normalized (a) growth rate Ω_i and (b) shifted real frequency Ω_r versus f [Eqs. (36) — (38)] for the (m, n) = (2, 0), (2, 1) and (3, 0) modes.

B. Discussion

As shown in Figs. 1-3, for any given mode there is a threshold value f_1 such that instability occurs for $f > f_1$. In addition, each mode has a second threshold $f_2 > f_1$ such that the instability is purely growing, i.e. $\mathrm{Re}\Omega = 0$, if $f > f_2$. If $f_2 = f_1$, the instability is always purely growing, but if $f_2 > f_1$ the instability is oscillatory in the range $f_1 < f < f_2$. A purely growing instability mode, in the limit $\omega\tau_d \ll 1$ which we have considered, may be expected to be particularly dangerous to beam integrity. The values of f_1 and f_2 are tabulated, for each of the modes in Table 1.

Among the m = 0 modes the n = 2 hollowing mode would appear to be particularly dangerous because of its low instability threshold; however the instability is oscillatory except at a very high return current fraction, $f_2 = 0.95$. The n = 1 sausage mode has a somewhat higher instability threshold, $f_1 = 0.5$, but is purely growing whenever it is unstable, and has the largest growth rate of any mode over the range $0.6 \lesssim f < 1$. There are two distinct n = 3 branches, one of which is purely growing, but with the large instability threshold $f_1 = 0.95$, while the other is always oscillatory.

Among the m = 1 modes, the n = 0 hose mode (which has been studied more extensively in Refs. 3-7) would appear to be by far the most dangerous. It is unstable for any value of $f > 0$, is always purely growing (when $\omega\tau_d \ll 1$ and thus resistive phase lag effects are neglected, as is done throughout this paper), and has the largest growth rate of any m = 1 mode except at very large values of f. The n = 1 and n = 2 modes are oscillatory up to large values of f. Both of these modes turn on at $f_1 = 0.5$, and have the same growth rate in the regime where both are oscillatory.

The m = 2 modes are elliptical distortions which at large amplitude tend to split the beam in two. Both the (m,n) = (2,0) and (2,1) modes are purely

growing whenever they are unstable, but the threshold for both modes is rather high, $f_1 = 0.75$ and 0.87 respectively. The $(m,n) = (3,0)$ filamentation mode, on the other hand, turns on at the surprisingly low threshold $f_1 = 0.53$, but is purely growing only at very large f.

Of all the modes studied, the dispersion properties would appear to single out the hose as most dangerous, with two of the axisymmetric modes, $m = 0$, $n = 1, 2$, next. This is in accord with the conventional wisdom that hose is the most dangerous mode. On the other hand, the hose mode in a well-prepared beam must grow out of small-amplitude noise, whereas the axisymmetric modes may be initially excited at much larger amplitude, due to the violent pinch-down of the beam head[10,11], or to the axisymmetric oscillations of a beam which is mismatched at injection. Thus experimental study of all three of these modes, as well as further theoretical investigation using simulation techniques to model the beam realistically, would appear to be warranted.

Table I

Mode Numbers			
m	n	f_1	f_2
0	1	0.5	0.5
0	2	0.38	0.95
0	3	0.45	1
0	3	0.95	0.95
1	0	0	0
1	1	0.5	0.89
1	2	0.5	0.96
2	0	0.75	0.75
2	1	0.87	0.87
3	0	0.53	0.96

Threshold values of fractional current neutralization f for the various modes: $f > f_1$ is the condition for instability, and $f > f_2$ is the condition for pure growth.

C. Concluding Remarks

In this paper we have presented a stability analysis of all of the first nine modes ($1 \leq m + n \leq 3$) of a beam propagating in a resistive plasma. The results are based on an exact Vlasov analysis, which is carried out in closed form. This is possible because of two principal restrictions: we considered only beam equilibria in which $J_{bo}(r)$ and $J_{po}(r)$ are flat, and we considered only the case $\omega\tau_d \ll 1$. These two restrictions are compatible with each other: in the regime $\omega\tau_d \ll 1$ the instability is driven only by the presence of an equilibrium return current $I_p \neq 0$, and this mechanism is only moderately sensitive to the profile $J_{bo}(r)$. The analysis is obviously incomplete. Modes with $\omega\tau_d \sim 1$ are also important, and because these modes are driven additionally by resistive phase lags between perturbed beam current and perturbed plasma eddy currents, they can in some cases become unstable at lower values of I_p and have larger growth rates. However these modes are also sensitive to the stabilizing effect of phase mixing among particles of different betatron frequency, and therefore to the profiles of $J_{bo}(r)$ and $J_{po}(r)$. Thus, if one is to treat these instabilities over the full range of $\omega\tau_d$, it is important to use realistic beam profiles and not to use models that eliminate or misrepresent phase mixing. A complete Vlasov analysis would of course be ideal, but no such analysis has been presented to date for beams with rounded profiles.[12] Instead, several phenomenological techniques have been developed to model phase mixing and beam profile dependence of the hose[3,4,6,7] and sausage[8,6] modes, but these techniques have not been adapted to the higher modes discussed in this paper, as yet.

One other restriction of the present model should be mentioned. We have implicitly assumed that the conductivity channel $\sigma(r)$ is pre-formed before the arrival of the beam and is uninfluenced by the passage of the beam. In fact, for a high-current beam injected into a neutral or weakly ionized gas, augmentation

of the conductivity as a result of ionization and heating by the beam can have a strong stabilizing effect,[6] and should be treated self-consistently with the beam dynamics in these situations.

Acknowledgments

This research was supported in part by the Independent Research Fund at the Naval Surface Weapons Center and in part by Defense Advanced Research Projects Agency (DOD) under ARPA Orders No. 3718, Amendment 32, and No. 4395, Amendment 1.

References

1. M. N. Rosenbluth, Phys. Fluids 3, 932 (1960).
2. S. Weinberg, J. Math Phys. 8, 614 (1967).
3. E. P. Lee, Phys. Fluids 21, 1327 (1978).
4. H. S. Uhm and M. Lampe, Phys. Fluids 23, 1574 (1980).
5. H. S. Uhm and M. Lampe, Phys. Fluids 24, 1553 (1981).
6. G. Joyce, M. Lampe, W. M. Sharp, and H. S. Uhm, 4th Intl. Topical Conference on High Power Electron and Ion Beam Research and Technology, Ecole Polytechnique, Palaiseau, France, in press (1981).
7. W. M. Sharp, M. Lampe and H. S. Uhm, "Multi-Component Model of the Resistive Hose Instability", Naval Research Laboratory Memorandum Report, in press (1982).
8. E. P. Lee, Lawrence Livermore National Laboratory Report UCID-18940 (1981).
9. In Refs. 4 and 5, γ_b was incorrectly defined as $(1 - v_z^2/c^2)^{-1/2}$. The definition in the present paper is the correct one. However this correction does not otherwise modify the content of Refs. 4 and 5.
10. W. M. Sharp and M. Lampe, Phys. Fluids 23, 2383 (1980).
11. E. P. Lee, Lawrence Livermore National Laboratory Report UCID-18768 (1980).
12. However it is shown in Ref. 7 that the multi-component model of the hose instability, developed in Refs. 6 and 7, is a very good approximation to the exact Vlasov result.

DISTRIBUTION LIST

1. Commander
   Naval Sea Systems Command
   Department of the Navy
   Washington, D.C. 20363
   Attn: NAVSEA 03H (Dr. C. F. Sharn)

2. Central Intelligence Agency
   P.O. Box 1925
   Washington, D.C. 20013
   Attn: Dr. C. Miller/OSI

3. Air Force Weapons Laboratory
   Kirtland Air Force Base
   Albuquerque, New Mexico 87117
   Attn: Lt. Col. J. H. Havey

4. U. S. Army Ballistics Research Laboratory
   Aberdeen Proving Ground, Maryland 21005
   Attn: Dr. D. Eccleshall (DRXBR-BM)

5. Ballistic Missile Defense Advanced Technology Center
   P.O. Box 1500
   Huntsville, Alabama 35807
   Attn: Dr. L. Havard (BMDSATC-1)

6. B-K Dynamics, Inc.
   15825 Shady Grove Road
   Rockville, Maryland 20850
   Attn: Mr. I. Kuhn

7. Intelcom Rad Tech.
   P.O. Box 81087
   San Diego, California 92138
   Attn: Mr. W. Selph

8. Lawrence Livermore National Laboratory
   University of California
   Livermore, California 94550
   Attn: Dr. R. J. Briggs
   Dr. T. Fessenden
   Dr. E. P. Lee
   Dr. F. Chambers
   Dr. S. Yu
   Dr. James W.-K. Mark, L-477
   Dr. W. Fauley
   Dr. H. L. Buchanon
   Dr. J. Masamitsu
   Dr. W. Barletta

9. Mission Research Corporation
735 State Street
Santa Barbara, California 93102
Attn: Dr. C. Longmire
Dr. N. Carron

10. National Bureau of Standards
Gaithersburg, Maryland 20760
Attn: Dr. Mark Wilson

11. Science Applications, Inc.
1200 Prospect Street
La Jolla, California 92037
Attn: Dr. M. P. Fricke
Dr. W. A. Woolson

12. Science Applications, Inc.
5 Palo Alto Square, Suite 200
Palo Alto, California 94304
Attn: Dr. R. R. Johnston
Dr. Leon Feinstein

13. Science Applications, Inc.
1651 Old Meadow Road
McLean, Virginia 22101
Attn: Mr. W. Chadsey

14. Science Applications, Inc.
8201 Capwell Drive
Oakland, California 94621
Attn: Dr. J. E. Reaugh

15. Naval Surface Weapons Center Detachment
White Oak Laboratory
Silver Spring, Maryland 20910
Attn: Mr. R. J. Biegalski
Dr. R. Cawley
Dr. J. W. Forbes
Dr. D. L. Love
Dr. C. M. Huddleston
Dr. G. E. Hudson
Mr. W. M. Hinckley
Mr. N. E. Scofield
Dr. E. C. Whitman
Dr. M. H. Cha
Dr. H. S. Uhm
Dr. R. Fiorito

16. C. S. Draper Laboratories
Cambridge, Massachusetts 02139
Attn: Dr. E. Olsson
Dr. L. Matson

17. M.I.T. Lincoln Laboratories
P.O. Box 73
Lexington, Massachusetts 02173
Attn: Dr. J. Salah

18. Physical Dynamics, Inc.
P.O. Box 1883
La Jolla, California 92038
Attn: Dr. K. Brueckner

19. Office of Naval Research
Department of the Navy
Arlington, Virginia 22217
Attn: Dr. W. J. Condell (Code 421)

20. Avco Everett Research Laboratory
2385 Revere Beach Pkwy
Everett, Massachusetts 02149
Attn: Dr. R. Patrick
Dr. Dennis Reilly
Dr. D. H. Douglas-Hamilton

21. Defense Technical Information Center
Cameron Station
5010 Duke Street
Alexandria, VA 22314 (2 copies)

22. Naval Research Laboratory
Washington, D.C. 20375
Attn:
M. Lampe - Code 4792 (50 copies)
M. Friedman - Code 4700.1
J. R. Greig - Code 4763
I. M. Vitkovitsky - Code 4770
J. B. Aviles - Code 4665
M. Haftel - Code 4665
T. Coffey - Code 4000
Superintendent, Plasma Physics Div. - Code 4700 (26 copies)
P. Sprangle - Code 4790
Library - Code 2628 (20 copies)
A. Ali - Code 4700.1
D. Book Code 4040
J. Boris - Code 4040
I. Haber - Code 4790
B. Hui - Code 4790
S. Kainer - Code 4790
G. Joyce - Code 4790
D. Murphy - Code 4763
A. Robson - Code 4760
D. Colombant - Code 4790
M. Picone - Code 4040
M. Raleigh - Code 4760
R. Pechacek - Code 4763

23. Defense Advanced Research Projects Agency
1400 Wilson Blvd.
Arlington, VA 22209
Attn: Dr. J. Mangano
Dr. J. Bayless

24. JAYCOR
5705A General Washington Drive
Alexandria, VA 22312
Attn: Dr. D. Tidman
Dr. R. Hubbard
Dr. J. Guillory
Dr. S. Slinker

25. JAYCOR
Naval Research Laboratory
Washington, D.C. 20375
Attn: Dr. R. Fernsler - Code 4763
Dr. S. Goldstein - Code 4770

26. SAI
Naval Research Laboratory
Washington, D.C. 20375
Attn: A. Drobot - Code 4790
W. Sharp - Code 4790

27. Physics International, Inc.
2700 Merced Street
San Leandro, CA.
Attn: Dr. E. Goldman

28. Mission Research Corp.
1400 San Mateo, S.E.
Albuquerque, NM 87108
Attn: Dr. Brendan Godfrey

29. Princeton University
Plasma Physics Laboratory
Princeton, NJ 08540
Attn: Dr. Francis Perkins, Jr.

30. McDonnell Douglas Research Laboratories
Dept. 223, Bldg. 33, Level 45
Box 516
St. Louis, MO 63166
Attn: Dr. Michael Greenspan

31. Cornell University
Ithaca, NY 14853
Attn: Prof. David Hammer

32. Sandia Laboratories
Albuquerque, NM 87185
Attn: Dr. Bruce Miller
Dr. Barbara Epstein
Dr. John Freeman

33. University of California
Physics Department
Irvine, CA 92717
Attn: Dr. Gregory Benford

34. Beers Associates Inc.
Att: Dr. Douglas Strickland
P.O. Box 2549
Reston Va. 22090

35. Air Force Weapons Laboratory
Kirtland Air Force Base
Albuquerque, NM 87117
Attn:
D. Straw (AFWL/NTYP)
R. Lemke (AFWL/NTYP)
C. Clark (AFWL/NTYP)
W. Baker (AFWL/NTYP)

36. R&D Associates
P.O. Box 9695
Marina del Rey, CA 90291

37. Pulse Sciences, Inc.
1615 Broadway - Suite 610
Oakland, CA 94612
Attn: Dr. Sidney Putman

38. Los Alamos National Scientific Laboratory
P.O. Box 1663
Los Alamos, NM 87545
Attn: Dr. L. Thode
Dr. A. B. Newberger, X-3, MS-608
Dr. M. A. Mostrom, MS-608
Dr. T. P. Starke
Dr. H. Dogliani

39. Western Research Corp
8616 Commerce Ave.
San Diego, CA 92121
Attn: Dr. Frank Felber

40. Dr. J. M. Dolique
Laboratoire de Physique des Plasmas
Universite' de Grenoble I
B.P. 53X
38041 Grenoble Cedex
FRANCE

41. CEN Saclay
D.P.C. Bab 22
B.P. No. 2
91191 Gif-sur-Yvette
FRANCE
Attn: Dr. Babuel-Peyrissac

42. University of Maryland
Physics Department
College Park, MD 20742
Attn: Dr. Y. C. Lee
Dr. C. Grebogi

43. Rutherford Laboratory
Chilton, Didcot
Oxon OX11 OQX
United Kingdom
Attn: Dr. D. V. Bugg

44. Karacsony Fanos
Center for Theoret. Physics
University of Cluj
3.400 CLUJ-NAPOCA
ROMANIA

45. Maxwell Laboratories, Inc.
8835 Balboa Ave.
San Diego, CA 92123
Attn: Dr. Nino Pereira

46. Fraunhofer-Gesellschaft
Institut fur Naturwissenschaftlich-Technische Trendanalysen (INT)
Appelsgarten 2
5350 Euskirchen/Rhld.
West-Germany
Attn: Dr. A. Knoth

47. Dr. A. S. Paithankar
Bhabha Atomic Research Centre
Electronics & Instrumentation Group,
Plasma Physics Section
PRIP Shed. Trombay
Bombay-400 085. INDIA